REFERENCES

[1] D. W. Kammler, "Calculation of characteristic admittances and coupling coefficients for strip transmission lines," *IEEE Trans. Microwave Theory Tech.*, vol. MTT-16, pp. 925–937, Nov. 1968.

[2] R. Mittra, *Computer Techniques for Electromagnetics, Vol. 7*. New York: Pergamon, 1973, ch. 6.

[3] R. E. Collin, *Field Theory of Guided Waves*. New York: McGraw-Hill, 1960, pp. 139–143.

[4] F. C. Yang and K. S. H. Lee, "Impedance of a two conical plate transmission line," Sensor and Simulation Note 221, Nov. 1976.

[5] I. S. Gradshteyn and I. M. Ryzhix, *Tables of Integrals, Series and Products*. New York: Academic Press, 1965, p. 84.

[6] M. Abromowitz and I. A. Stegun, *Handbook of Mathematical Functions (Applied Mathematics Series 55)*. National Bureau of Standards, 1970.

[7] P. F. Byrd and M. D. Friedman, *Handbook of Elliptic Integrals for Engineers and Scientists*. New York: Springer, 1971, p. 12.

[8] F. Assadourian and E. Rimai, "Simplified theory of microstrip transmission system," *Proc. IRE*, vol. 40, pp. 1651–1657, Dec. 1952.

[9] M. Kumar and B. N. Das, "Coupled transmission lines," *IEEE Trans. Microwave Theory Tech.*, vol. MTT-25, pp. 7–11, Jan. 1977.

[10] R. W. Breithaupt, "Conductance data for offset series slots in stripline," *IEEE Trans. Microwave Theory Tech.*, vol. MTT-16, p. 969, Nov. 1968.

Field and Network Analysis of Interacting Step Discontinuities in Planar Dielectric Waveguides

TULLIO E. ROZZI, SENIOR MEMBER, IEEE, AND GERARD H. IN'T VELD

Abstract—**Planar dielectric waveguides play an important role in electrooptics and at millimeter frequencies. In many laser configurations and integrated optical components, grooves are etched in the planar surface or overlays are deposited on it. The step is an idealization of such a discontinuity. Step discontinuities are seldom isolated. Mostly a cascade is employed. The aim of this paper is to derive, from a rigorous field analysis, an accurate finite network description for such cascades, either finite or infinite, periodic or aperiodic, which takes account also of the continuous spectrum. Numerical examples are given.**

I. INTRODUCTION

THE ANALYSIS of discontinuities in open dielectric waveguides is still in its infancy, and very few techniques are known [1]. In this paper we study an important class of discontinuities, namely, the cascade of steps in a planar dielectric waveguide, such as shown in Fig. 1. This is a basic configuration occurring in passive and active components for integrated optics and optical communications, such as the grating coupler, the transformer/echelon, and the distributed feedback laser. Corrugated dielectric waveguides are also used for millimeter waves and as microwave antenna feeds. Various approximations have been introduced for dealing with small discontinuities between monomode guides (see, for instance, [1]–[4]). The infinite periodic case has been treated extensively and rigorously (see, for instance, [5] for a most comprehensive list of references (287), as well as [6]). The problem of an isolated, large step between two multimode waveguides has been treated rigorously [7]. The general problem of arbitrarily large, aperiodic interacting steps is unsolved up to date. However, the optimum performance of various

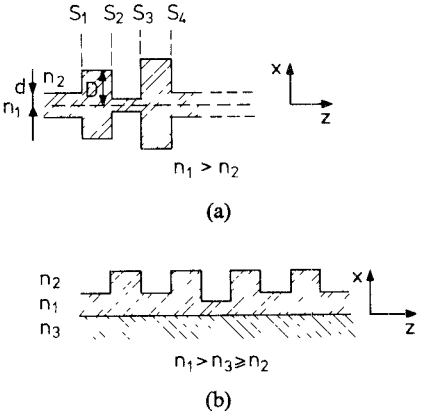

Fig. 1. Cascade of steps in a planar dielectric waveguide. (a) Cascade of symmetric steps. (b) Cascade of asymmetric steps.

Manuscript received June 6, 1978; revised October 30, 1978.

T. E. Rozzi was with Philips Research Laboratories, Eindhoven, The Netherlands. He is now with the Department of Electrical Engineering and Electronics, The University of Liverpool, Liverpool, England.

G. H. in't Veld is with Philips Research Laboratories, Eindhoven, The Netherlands.

0018-9480/79/0400-0303$00.75

components is dependent, for instance, upon optimizing the spacing between discontinuities and minimizing (or maximizing) radiation at certain angles. It is, therefore, worthwhile to develop an accurate analysis of general validity. Fig. 1 illustrates the basic geometry. The structure is uniform in the y direction, not shown. Material losses are not considered in this context, although this is not an essential restriction.

An open dielectric waveguide allows, besides a finite number of surface waves, a continuum of modes. The modes within a finite range of the continuum are propagating; the rest represent localized energy storage (reactive modes). A surface wave incident from the left is scattered by the step S_1 in all the surface modes allowed at either side of S_1 as well as in the modes of the continuous spectrum. After propagating up to S_2, the surface waves and the propagating part of the continuous spectrum are again scattered by the second step, so that interference between S_1 and S_2 takes place. The reactive part of the continuous spectrum, being nonpropagating, is virtually localized to the neighborhood of the discontinuity. The problem involves two levels of complexity, depending on whether we disregard or consider interaction via propagating continuous modes. In the former case, the field problem of a single step is first solved by means of the approach of [7]. This analysis results in a multiport network which describes how the junction is seen by the surface waves: a port corresponds to each surface wave at each side of the step. The cascade of interacting steps is then described by a model consisting of discrete multiports connected by transmission lines: one pair of ports and one transmission line per surface wave. This is analogous to the representation of interacting discontinuities in closed waveguides [8]. A more complex situation arises for cascaded discontinuities in weakly guiding structures, but also for a large double-step discontinuity, where the propagating continuous modes excited at one step "see" the adjacent step, and it is impossible to ignore their interaction. The picture of the step as a discrete multiport is no longer adequate. A discontinuity is now intrinsically a "generalized multiport" (GM), having a finite number of discrete ports (the surface waves), plus a continuum of ports (the continuous spectrum).

Although the GM retains many of the formal properties of an ordinary multiport, it is no longer amenable to the methods of finite network analysis and, as such, is no longer useful. This difficulty is surmounted by giving up the simple model of individual-mode propagation along uncoupled, parallel transmission lines between successive discontinuities.

Introducing a new representation of each length of waveguide between successive discontinuities, including the discontinuities at either end, reduces it to a discrete $2N$-port network. All the N pairs of ports are mutually coupled, but the above model is now amenable to ordinary network analysis. The equivalence of the network approach to a Ritz–Galerkin variational solution will presently become apparent.

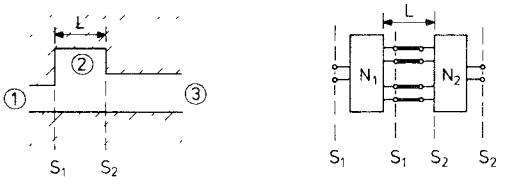

Fig. 2. (a) Double-step discontinuity in a closed homogeneous waveguide. (b) Network representation.

In the following, we will consider slab waveguides excited by even TE waves. This particularization considerably simplifies the modal spectrum with no loss of generality to the principles involved. The necessary modifications for the general multilayer waveguide and the TM case are described elsewhere [9], [10].

II. Integral Equations for the Double-Step Discontinuity

Fig. 2(a) shows a double-step discontinuity in a closed homogeneous waveguide. The field problem is transformed into the network problem of Fig. 2(b). Each step is represented by a multiport connected to the other by a finite and generally small number of transmission lines, one for each mode, either propagating or cutoff, which causes nonnegligible interaction (which we define, as in [8], an "accessible" mode). If enough modes are considered accessible, the field problem of a step can be treated in isolation. Hence the step and the intervening length of waveguide are the "building blocks" of the cascade.

Consider now the case of a double-step discontinuity in the slab waveguide of Fig. 3(a) (groove) or of its counterpart of Fig. 3(b) (rib). As long as interaction takes place mainly via the surface waves, as in Fig. 3(b) with n_1 considerably larger than n_2, so that we can disregard interaction via the continuous spectrum, the representation of Fig. 2(b) still applies. For Fig. 3(a), however, with $n_1 \gtrsim n_2$, considerable radiation takes place at the step, and the familiar representation no longer holds. Propagating continuous modes, while being accessible, cannot be modeled by means of a finite number of transmission lines. In order to proceed, we must first retreat one step and reformulate the field problem.

Consider the situation where slabs 1 and 3 of Fig. 3(a) are semi-infinite. The relationship between the transverse (y-directed) electric field E and the transverse (x-directed) magnetic field H at $z=0^-$ is [7]

$$E(x,0) = -\int_0^\infty \mathcal{Z}_1(x,x')[-H(x',0)]\,dx' \equiv -\hat{Z}_1\cdot[-H(x,0)] \quad (1)$$

where

$$\mathcal{Z}_1(x,x') = \sum_{n=1}^{\bar{n}_1} z_{0n}\varphi_n(x)\varphi_n(x') + \int_0^\infty z_0(\rho)\varphi(x,\rho)\varphi(x',\rho)\,d\rho \quad (2)$$

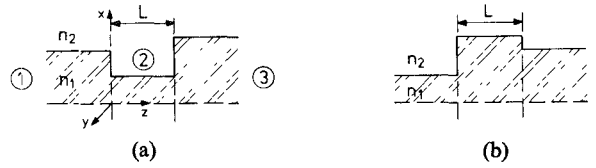

(a) (b)

Fig. 3. Double-step discontinuity in a planar dielectric waveguide. (a) Groove. (b) Rib.

is the Green's impedance function of the semi-infinite slab 1. $\varphi_1 \cdots \varphi_{\bar{n}1}$ are the modal fields of the $\bar{n}_1$ surface waves with characteristic impedances $z_{01} \cdots z_{0n_1}$; $\varphi(x,\rho)$ represents a component of the continuum with characteristic impedance $z_0(\rho)$. Similarly, at $z=L$, we have

$$E(x,L) \equiv \hat{Z}_z \cdot [-H(x,L)] \tag{3}$$

where

$$\mathfrak{Z}_2(x,x') = \sum_{n=1}^{\bar{n}_2} z'_{0n}\psi_n(x)\psi_n(x') + \int_0^\infty z_0(\rho)\psi(x,\rho)\psi(x',\rho)\,d\rho. \tag{4}$$

The various quantities occurring in (4) resemble those occurring in (2). In particular, $z_0(\rho)$ is the same for both slabs. If E is identified with an abstract "voltage" and $-H$ with an abstract "current," then $\hat{Z}_{1,2}$ are driving-point impedance operators of the semi-infinite slabs 1,3. We now need a link between the fields at $z=0$ and $z=L$, which represents the effect of the finite length of slab waveguide between the steps. Let $\Phi_k(x)$ $(1 \leqslant k \leqslant \bar{k})$ denote the surface waves in region 2, having propagation constants Γ_k and characteristic impedances (TE modes)

$$Z_{0k} = \frac{j\omega\mu_0}{\Gamma_k} \quad (\Gamma_k = j\beta_k) \tag{5}$$

and let $\varphi(x,\rho)$ denote a component of the continuous spectrum with propagation constant $\Gamma(\rho)$ and characteristic impedance

$$Z(\rho) = \frac{j\omega\mu_0}{\Gamma(\rho)} = \frac{\omega\mu_0}{\sqrt{n_2^2k_0^2-\rho^2}}, \qquad \text{for } \rho < n_2k_0$$

$$= \frac{j\omega\mu_0}{\sqrt{\rho^2-n_2^2k_0^2}}, \qquad \text{for } \rho > n_2k_0. \tag{6}$$

ρ is the transverse wavenumber in the air region, so that $\rho^2+\beta^2 = n_2^2k_0^2$, $(k_0=\omega/c)$. When a magnetic wall is placed at $z=L$ $(H(x,L)=0)$, the transverse electric field $E(x,0)$ excited by $H(x,0)$ is

$$E(x,0) = \hat{Z}_{11} \cdot [-H(x,0)]$$

$$= \int_0^\infty dx' \left\{ \sum_{k=1}^{\bar{k}} Z_{0k} \coth(\Gamma_k L)\Phi_k(x)\Phi_k(x') + \int_0^\infty d\rho\, Z_0(\rho) \coth(\Gamma(\rho)L)\Phi(x,\rho)\Phi(x',\rho) \right\} \cdot [-H(x',0)]. \tag{7}$$

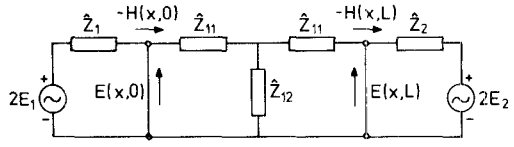

Fig. 4. Abstract network representation of the integral equations for the double step.

This expression[1] is the operator form of the driving point impedance of an open-circuit stub. Moreover, under the same boundary conditions, we have

$$E(x,0) = -\hat{Z}_{12} \cdot [-H(x,L)] \tag{8}$$

where $\hat{Z}_{12}$ is derived from (7) by replacing the coth function by csch. When a magnetic wall is placed at $z=0$ and $E(x,0)$ is set equal to zero, we have by symmetry

$$E(x,L) = -\hat{Z}_{11} \cdot [-H(x,L)] \tag{9}$$

and by reciprocity

$$E(x,L) = \hat{Z}_{12} \cdot [-H(x,0)]. \tag{10}$$

The above equations (7)–(10) can be combined in a "two-port" Green's open-circuit impedance operator for the length of waveguide $0 \leqslant z \leqslant L$:

$$\begin{pmatrix} E(x,0) \\ E(x,L) \end{pmatrix} = \begin{bmatrix} \hat{Z}_{11} & -\hat{Z}_{12} \\ \hat{Z}_{12} & -\hat{Z}_{11} \end{bmatrix} \cdot \begin{pmatrix} -H(x,0) \\ -H(x,L) \end{pmatrix}. \tag{11}$$

Continuity of the transverse fields at $z=0$, L yields two coupled integral equations for $H(x,0), H(x,L)$ which completely describe the problem.

Their abstract network representation is shown in Fig. 4, where the positive current convention is that from left to right. From this figure, the relationships between the field incident from the left at $z=0$

$$E_1(x,0) = \sum_{n=1}^{\bar{n}_1} a_n\varphi_n(x) \tag{12a}$$

and that incident from the right at $z=L$

$$E_2(x,L) = \sum_{n=1}^{\bar{n}_2} a_{\bar{n}_1+n}\psi_n(x) \tag{12b}$$

and the total fields at $z=0$, L are found to be

$$E(x,0) = 2E_1(x,0) - \hat{Z}_1 \cdot [-H(x,0)] \tag{13a}$$

$$E(x,L) = 2E_2(x,L) + \hat{Z}_2 \cdot [-H(x,L)]. \tag{13b}$$

Hence, from (11) and (13), the integral equations describ-

[1]The integrand has no branch line singularities but only poles for $\beta(\rho)\cdot L = m\pi$. These are avoided by means of small indentations on the upper half-plane ("small" losses). One such pole contributes a term

$$\epsilon_m(\omega\mu_0/\rho_m)(\pi/L)\Phi(x,\rho_m)\Phi(x',\rho_m)$$

$$\left(\epsilon_0 = \tfrac{1}{2},\ \epsilon_{m\neq 0} = 1,\ \rho_m = \sqrt{n_2^2k_0^2-(m\pi/L)^2}\right)$$

to the Green's function.

ing the scattering properties of the double step are

$$\begin{pmatrix} E_1(x,0) \\ -E_2(x,L) \end{pmatrix} = \frac{1}{2}\left[\begin{array}{c|c} \hat{Z}_1+\hat{Z}_{11} & -\hat{Z}_{12} \\ \hline -\hat{Z}_{12} & \hat{Z}_2+\hat{Z}_{11} \end{array}\right]\cdot\begin{pmatrix} -H(x,0) \\ -H(x,L) \end{pmatrix}. \tag{14}$$

For the double step in a closed homogeneous waveguide, decoupling of the integral equations takes place essentially by replacing the off-diagonal terms of the matrix in (14) by independent sources. This approach is feasible in as much as interaction between adjacent steps can be described effectively by means of a few parallel uncoupled discrete transmission lines. Hence, the network representation of Fig. 2(b) results.

In the present situation, this is no longer possible due to the propagating continuous modes. We must consider, therefore, the whole length of waveguide between two successive steps, including the steps, as the building block of the cascade.

III. Transformer Embedding and Finite Network Representation

The abstract representation of the double step given in Fig. 4 is not an actual equivalent network, amenable to ordinary network analysis, but it is our aim to derive such a network. The integral equation for the single step can be reduced to a finite matrix equation by means of a discrete sequence of functions (not necessarily orthonormal, but belonging to a complete set) truncated after N terms. This amounts in fact to the Ritz–Galerkin variational approach [11].

For the symmetric TE case, for instance, an appropriate orthonormal "basis" of functions for representing the slab modes is given by

$$\left\{ \mathfrak{L}_m(x) = \frac{1}{\sqrt{x_0}} \exp(-x/2x_0) L_{m-1}\left(\frac{x}{x_0}\right), \quad m = 1 \cdots N \right\} \tag{15}$$

where L denotes the Laguerre polynomial and x_0 is a scale factor chosen so as to optimize the convergence of the representation for any finite truncation N [7]. Introducing such a sequence at $z=0$, we expand the slab modes in region 1 as[2]

$$\psi_n(x) = \sum_{m=1}^{N} P_{mn}\mathfrak{L}_m(x) \tag{16a}$$

$$\varphi(x,\rho) = \sum_{m=1}^{N} P_{m\rho}\mathfrak{L}_m(x) \tag{16b}$$

where

$$P_{mn} = \langle \mathfrak{L}_m, \varphi_n \rangle = \int_0^\infty \mathfrak{L}_m(x)\varphi_n(x)\,dx \tag{17a}$$

[2]As $N\to\infty$, (16a) converges "in the mean," and (16b) only in a distributional sense. This relates to the delta function normalization of the continuous modes and to the finiteness of energy, which is defined under an integral sign. As apparent from (18), classical convergence of (16b) is not required.

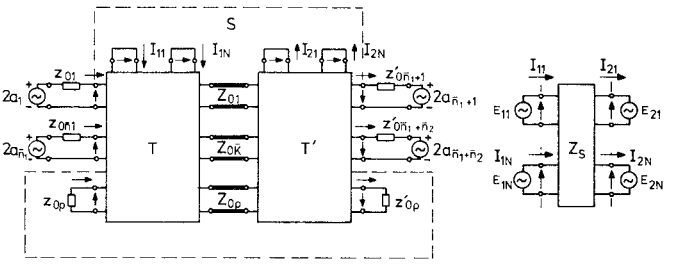

Fig. 5. Finite network representation of the double step.

$$P_{m\rho} \equiv P_m(\rho) = \langle \mathfrak{L}_m, \varphi_\rho \rangle = \int_0^\infty \mathfrak{L}_m(x)\varphi(x,\rho)\,dx. \tag{17b}$$

Using (15) as a basis, (2) becomes[3]

$$\boldsymbol{Z}_1 = \sum_{n=1}^{\bar{n}_1} z_{0n}\boldsymbol{P}_n\boldsymbol{P}_n^t + \int_0^\infty d\rho\, z_0(\rho)\boldsymbol{P}(\rho)\boldsymbol{P}^t(\rho) \tag{18}$$

where $\boldsymbol{P}_n$ is the vector with components given by (17a). We can combine the latter so as to define a rectangular $(\bar{n}_1 \times N)$ transformer matrix

$$\boldsymbol{T}_d^t = \begin{pmatrix} P_{11} & \cdots & P_{N1} \\ P_{1\bar{n}_1} & \cdots & P_{N,\bar{n}_1} \end{pmatrix}. \tag{19}$$

The finite sum in (18) can be written as

$$\boldsymbol{T}_d^t \cdot z_{0d} \cdot \boldsymbol{T}_d \tag{20}$$

where $z_{0d} = \text{diag}\,(z_{01}, \cdots, z_{0\bar{n}_1})$, which is the familiar expression of a transformer embedding of an impedance matrix (see Fig. 5). In analogous fashion, we introduce the $N \times 1$ transformer

$$\boldsymbol{T}_\rho = (P_{1\rho} \cdots P_{N\rho})^t \tag{21}$$

and write (18) as

$$\boldsymbol{Z}_1 = (\boldsymbol{T}_d^t \cdot \boldsymbol{T}_\rho)\cdot\begin{pmatrix} z_{0d} & \cdot \\ \cdot & z_{0\rho} \end{pmatrix}\cdot\begin{pmatrix} \boldsymbol{T}_d \\ \boldsymbol{T}_\rho \end{pmatrix} \tag{22}$$

where the dot product must be understood in the sense indicated in (18), partly as an ordinary matrix multiplication, partly as an integral over the product of scalar functions.

The resulting $N \times N$-matrix (18) can be interpreted as the impedance of an ordinary N-port, which approximates the field problem in the Ritz–Galerkin sense and is amenable to ordinary network analysis. The projections of the surface-wave modes of region 2 onto the basis (15) are given by

$$A_{mk} = \langle \mathfrak{L}_m, \Phi_k \rangle \tag{23a}$$

where $0 \leqslant k \leqslant \bar{k}$, while those of the modes of the continuum are given by

$$A_{m\rho} = \langle \mathfrak{L}_m, \Phi_\rho \rangle. \tag{23b}$$

Moreover, let us introduce at $z = L$ another finite

[3]The superscript t denotes transposition.

sequence, similar to (15),

$$\left\{\bar{\mathcal{L}}_m(x)=\frac{1}{\sqrt{\bar{x}}}\exp(-x/2\bar{x})\,L_{m-1}\left(\frac{x}{\bar{x}}\right);m=1\cdots N\right\} \tag{24}$$

where $\bar{x}$ is a scale constant.

The projections of the modes of slabs 2 and 3 on the latter basis are given by

$$\begin{aligned}\bar{A}_{mk}&=\langle\bar{\mathcal{L}}_m,\Phi_k\rangle\\ \bar{A}_{m\rho}&=\langle\bar{\mathcal{L}}_m,\Phi_\rho\rangle\\ R_{mn}&=\langle\bar{\mathcal{L}}_m,\psi_n\rangle\\ R_{m\rho}&=\langle\bar{\mathcal{L}}_m,\psi_\rho\rangle\end{aligned} \tag{25}$$

which introduce two ideal transformers with ratio matrices

$$\boldsymbol{T}^t=(\boldsymbol{P}_1\cdots\boldsymbol{P}_{\bar{n}_1}\boldsymbol{P}_\rho\boldsymbol{A}_1\cdots\boldsymbol{A}_{\bar{k}}\boldsymbol{A}_\rho) \tag{26a}$$

$$\bar{\boldsymbol{T}}^t=(\bar{\boldsymbol{A}}_1\cdots\bar{\boldsymbol{A}}_{\bar{k}}\bar{\boldsymbol{A}}_\rho\boldsymbol{R}_1\cdots\boldsymbol{R}_{\bar{n}_2}\boldsymbol{R}_\rho). \tag{26b}$$

Using (17), (23), (25), and (26), the integral equation (14) for the double step becomes the matrix equation

$$\begin{pmatrix}\boldsymbol{E}_1\\ -\boldsymbol{E}_2\end{pmatrix}=\boldsymbol{Z}_S\begin{pmatrix}\boldsymbol{I}_1\\ \boldsymbol{I}_2\end{pmatrix} \tag{27}$$

where from (12) and (16a), we have

$$E_{1m}=\sum_{n=1}^{\bar{n}_1}a_nP_{mn} \tag{28a}$$

$$E_{2m}=\sum_{n=1}^{n_2}a_{\bar{n}_1+n}R_{mn}. \tag{28b}$$

$\boldsymbol{I}_1,\boldsymbol{I}_2$ corresponds to $-H(x,0)$, $-H(x,L)$:

$$\boldsymbol{Z}_S=\frac{1}{2}\begin{pmatrix}\boldsymbol{Z}_1+\boldsymbol{Z}_{11} & -\boldsymbol{Z}_{12}\\ -\boldsymbol{Z}_{12}^t & \boldsymbol{Z}_2+\boldsymbol{Z}_{11}\end{pmatrix} \tag{29}$$

where $\boldsymbol{Z}_1$ is defined in (18) and

$$\boldsymbol{Z}_{11}=\boldsymbol{T}^t\cdot\operatorname{diag}(Z_{01}\coth\Gamma_1L,\cdots,Z_{0k}\coth\Gamma_kL,Z_{0\rho}\coth\Gamma_\rho L)\cdot\boldsymbol{T} \tag{30}$$

the dot product being understood in the sense of (18). An analogous definition holds for $\boldsymbol{Z}_{22}$ with $\boldsymbol{T}$ replaced by $\boldsymbol{T}$. Moreover, we have

$$\boldsymbol{Z}_{12}=\boldsymbol{T}^t\cdot\operatorname{diag}(Z_{01}\operatorname{csch}\Gamma_1L,\cdots,Z_{0k}\operatorname{csch}\Gamma_kL,Z_{0\rho}\operatorname{csch}\Gamma_\rho L)\bar{\boldsymbol{T}}. \tag{31}$$

The network interpretation of (29) is shown in Fig. 5.

The normalized scattering matrix of the double step, as seen by the surface waves incident at either side, can be derived from the above figure. By definition, its element $\bar{S}_{kl}$ is given by the voltage wave appearing at port k for unit incidence at port l. This expression is, in fact, formally the same as for the single step [7]

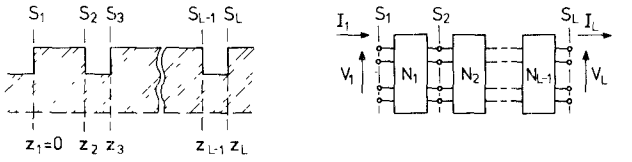

Fig. 6. (a) Cascade of multiple steps. (b) Its finite network representation.

$$\bar{S}_{kl}=\delta_{kl}-\sigma_k\sigma_l\sqrt{\bar{z}_{0k}\bar{z}_{0l}}\;\boldsymbol{U}_k^T\boldsymbol{Z}_s^{-1}\boldsymbol{U}_l \tag{32}$$

where

$$\begin{aligned}&\delta_{kl}=1\text{ if }k=l\qquad=0\text{ if }k\neq l\\ &1\leqslant k,l\leqslant\bar{n}_1+\bar{n}_2\\ &\sigma_k=\pm,\text{ as }k\gtrless\bar{n}_1\\ &\bar{z}_{0k}=\begin{cases}z_{0k} & :\ k\leqslant\bar{n}_1\\ z'_{0,k-\bar{n}_1} & :\ k>\bar{n}_1\end{cases}\\ &\boldsymbol{U}_k=\begin{cases}\boldsymbol{P}_k & :\ k\leqslant\bar{n}_1\\ \boldsymbol{P}_{k-\bar{n}_1} & :\ k>\bar{n}_1.\end{cases}\end{aligned}$$

IV. Cascade of Step Discontinuities

Having obtained the building blocks, i.e., the double-step discontinuity, we are now in a position to consider the cascade of steps such as shown in Fig. 6(a).

Within each uniform section, $E(x,z)$ and $-H(x,z)$ can be expressed at any point z as combinations of the surface waves and of the continuous spectrum of the section in question. The total transverse fields at z_i and z_{i+1} are related by

$$\begin{pmatrix}E(x,z_i)\\ -E(x,z_{i+1})\end{pmatrix}=\begin{pmatrix}\hat{Z}_{11}^{(i)} & -\hat{Z}_{12}^{(i)}\\ -\hat{Z}_{12}^{(i)} & \hat{Z}_{22}^{(i)}\end{pmatrix}\cdot\begin{pmatrix}-H(x,z_i)\\ -H(x,z_{i+1})\end{pmatrix} \tag{33}$$

where $\hat{Z}_{11}^{(i)}$, $\hat{Z}_{12}^{(i)}$, etc., are the two-port impedance operators for each section, as given by (11).

Introducing the ideal transformers T_i at z_i, we obtain the discrete equivalent network of Fig. 6(b).

Continuity of the transverse fields

$$\begin{aligned}E(x,z_i^-)&=E(x,z_i^+)\\ H(x,z_i^-)&=H(x,z_i^+)\end{aligned} \tag{34}$$

is translated into continuity of voltages and currents at the reference plane S_i. It should be emphasized that interaction via the propagating continuous spectrum between nonadjacent discontinuities is built into the model, as $E(x,z_i)$ represents the total transverse field at z_i. The analysis of the cascade is most conveniently carried out by cascade multiplication of the transfer matrices of the individual discrete networks $N_1\cdots N_L$. The transfer matrix relates voltages and currents at the left-hand-side ports to those at the right-hand side. If we denote by

$$\begin{pmatrix}\boldsymbol{Z}_{11} & -\boldsymbol{Z}_{12}\\ -\boldsymbol{Z}_{12}^t & \boldsymbol{Z}_{22}\end{pmatrix} \tag{35}$$

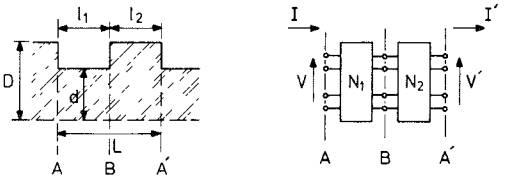

(a) (b)

Fig. 7. (a) Unit cell of the periodic cascade. (b) Its finite network representation.

the $2N$-impedance matrix of a discrete $2N$-port (with the sign convention of Fig. 6(b)), its transfer matrix is given by

$$\boldsymbol{M}=\left[\begin{array}{c|c} \boldsymbol{Z}_{11}\cdot(\boldsymbol{Z}_{12}^{t})^{-1} & -\left[\boldsymbol{Z}_{11}\cdot(\boldsymbol{Z}_{12}^{t})^{-1}\cdot\boldsymbol{Z}_{22}-\boldsymbol{Z}_{12}\right] \\ \hline (\boldsymbol{Z}_{12}^{t})^{-1} & -(\boldsymbol{Z}_{12}^{t})^{-1}\cdot\boldsymbol{Z}_{22} \end{array}\right]. \quad (36)$$

The inverse transformation, from $\boldsymbol{M}$ to $\boldsymbol{Z}$, is easily recovered. After the overall impedance matrix of the cascade has been obtained by network analysis, its scattering matrix, as seen by the $\bar{n}_1$ surface waves of the semi-infinite guide to the left of S_1 and $\bar{n}_i$ surface waves to the right of S_L, is given by (32). An important particular case arises when the cascade is infinite and periodic.

The unit cell of the periodic structure is shown in Fig. 7(a) and its finite, discrete equivalent network in Fig. 7(b). The relationship between voltages and currents at A and A' is

$$\begin{pmatrix} \boldsymbol{V} \\ \boldsymbol{I} \end{pmatrix}=\boldsymbol{M}_1\cdot\boldsymbol{M}_2\begin{pmatrix} \boldsymbol{V}' \\ \boldsymbol{I}' \end{pmatrix}. \quad (37)$$

The periodicity condition requires, however,

$$\begin{pmatrix} \boldsymbol{V}' \\ \boldsymbol{I}' \end{pmatrix}=e^{-\Gamma L}\begin{pmatrix} \boldsymbol{V} \\ \boldsymbol{I} \end{pmatrix} \quad (38)$$

where L is the length of the period and Γ is the propagation constant on the periodic structure. From (37) and (38) follows the (approximate) eigenvalue equation for the periodic structure:

$$\boldsymbol{M}_2^{-1}\boldsymbol{M}_1^{-1}\begin{pmatrix} \boldsymbol{V} \\ \boldsymbol{I} \end{pmatrix}=e^{-\Gamma L}\begin{pmatrix} \boldsymbol{V} \\ \boldsymbol{I} \end{pmatrix}. \quad (39)$$

Reciprocity implies that if Γ is an eigenvalue, so is $-\Gamma$. The transverse electric and magnetic fields, obtained from the corresponding independent eigenvectors, are

$$E^p(x)=\sum_{n=1}^{N} V_n^p\,\mathcal{E}_n(x) \quad (40a)$$

$$-H^p(x)=\sum_{n-1}^{N} I_n^p\,\mathcal{E}_n(x) \qquad (p=1\cdots N). \quad (40b)$$

If so required, the latter are easily expressed in terms of the spectrum of either waveguide of Fig. 7(a).

VII. Examples

The theory will not be illustrated by means of a few examples. These refer to slab structures excited by even TE waves. The required expressions of the mode functions, the Green's functions, and their discrete representation are given in [7]. Mathematical details on the computation of the integrals over the continuum as well as on the convergence of the discrete representation are also provided. Similar information for the TM case can be found in [9] and for the general multilayer case in [10].

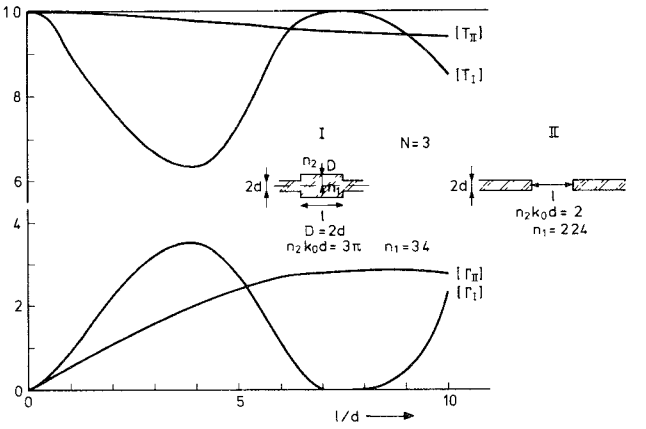

Fig. 8. Reflection and transmission coefficients of a symmetric double step versus relative separation.

A. Symmetric Double Step

The first example of Fig. 8 is a rib of AlGaAs in air excited by a surface wave incident from the left. For the given values of the parameters, only one surface wave can propagate in each section. The computation was carried out as described in Section IV using the discrete basis (15), truncated after three terms ($N=3$). Inclusion of additional terms produced only a very slight change in the characteristics.

In the figure the reflection coefficient Γ and transmission coefficient T_{12} are plotted versus the relative spacing $1/d$. Radiation losses for this configuration are virtually negligible, and the rib behaves almost like a resonator in closed waveguide. The above behavior contrasts with that of the second case of Fig. 8, namely an air gap between two collinear semi-infinite slabs. This is the degenerate case of the rib for $D=0$. The surface wave in the mid-region disappears, while the continuous spectrum of the slab becomes that of an homogeneous air region.

Radiation losses here are obviously high, and there is a fair amount of coupling between the slabs, which decreases only slowly with increasing spacing. The reflection coefficient, on the other hand, approaches that of a single semi-infinite slab radiating in air, as is to be expected.

B. The Quarter-Wave Transformer

Fig. 9 shows the counterpart of a classical configuration in microwave techniques, namely, a ten-to-one quarter-wave transformer. For the given values of the parameters, all three sections are monomode. Furthermore, the electrical length of the midsection is a quarter-wavelength at a point within the region of interest, and its thickness is chosen so that the impedance matching condition is satisfied. An obvious and simple approximation for this struc-

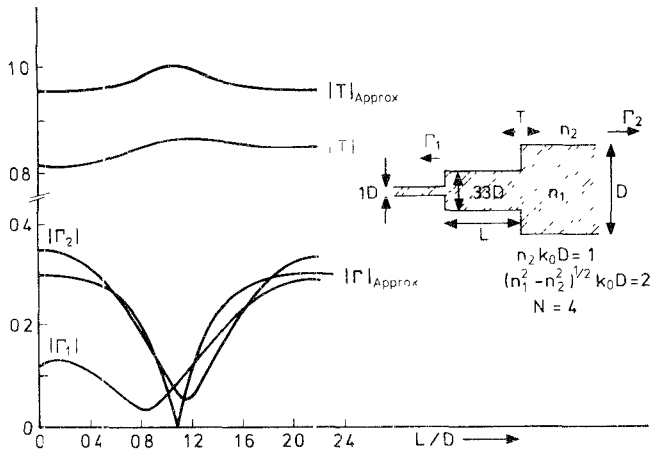

Fig. 9. The (not so) ideal quarter-wave transformer.

TABLE I
CONVERGENCE OF THE PROPAGATION CONSTANT OF THE INFINITE PERIODIC STRUCTURE OF FIG. 7

$n_2 k_0 d=1$; $D/d=2$; $l_1/d=l_2/d=1$; $(n_1^2-n_2^2)^{\frac{1}{2}} k_0 d=2$;

$B_1 = 2.147$ $B_2 = 1.330$ $\beta = 2.065$
$b = 1.985$

N	$Re(\beta_1)$	$Im(\beta_1)$
1	2.185	0
3	2.242	- 0.126
4	2.169	- 0.174
6	2.151	- 0.155
7	2.129	- 0.173
8	2.134	- 0.170

ture is obtained by treating it as a cascade of lossless transmission lines, disregarding mode conversion at the steps. Transmission and reflection coefficients in this approximation (T_{approx} and Γ_{approx}) are contrasted in the figure with the result of a fourth-order variational solution, carried out as described in Section IV, taking account of losses and of interaction. The behavior of the reflection coefficient from the left, Γ_1, is due to the fact that the surface wave is less well guided in the thin slab. This effect is felt particularly at short spacings. The effect of losses on the reflection minima and the transmission coefficient is also evident.

C. Infinite Periodic Structure

The unit cell of an infinite periodic structure is shown in Fig. 7(a). Table I shows the convergence of the propagation constant β_1 of the first mode of such a periodic structure with increasing order of the discrete representation.

For the sake of comparison, the propagation constants B_1, B_2 of the two surface waves of the thicker slab section and b of the thinner section are also given.

From simple transmission-line considerations, an estimate of the propagation constant, strictly speaking only valid for monomode slab sections, is

$$\beta \simeq \frac{1}{L} \cos^{-1}\left[\cos Bl_1 \cos bl_2 - \frac{1}{2}\left(\frac{B}{b} + \frac{b}{B}\right) \sin Bl_1 \sin bl_2\right]. \tag{41}$$

Hence, the similarity between $Re(\beta_1)$ and B_1 is hardly surprising. Owing to the multimode character of thicker slabs, however, the general behavior of the eigenvalues is rather complicated.

VIII. CONCLUSIONS

In conclusion, a general analysis technique has been outlined for cascaded step discontinuities in dielectric waveguides. The key point is transforming the field problem, which involves a continuous as well as a discrete spectrum, into a finite discrete network problem by means of an appropriate discrete representation. The discrete network is then amenable to standard network analysis.

Numerical examples are presented for the symmetric slab waveguide. For the general multilayer waveguide, the computational details differ, but the concepts involved remain the same. The possibility of approximating continuous transitions by cascaded discrete steps deserves further attention.

REFERENCES

[1] D. Marcuse, *Light Transmission Optics*. New York: Van Nostrand, 1972, ch. 9.
[2] C. C. Ghizoni, J. M. Ballantyne, and C. L. Tang, "Theory of optical waveguide d.f.b. lasers: A Green's function approach," *IEEE J. Quantum Electron.*, vol. QE-13, pp. 843–847, Oct. 1977.
[3] K. Ogawa, F. J. Rosenbaum, and W. S. C. Chang, "Scattering from discontinuities in thin film optical waveguides," unpublished.
[4] K. Ogawa, W. S. C. Chang, B. L. Sopori, and F. J. Rosenbaum, "A theoretical analysis of etched grating couplers for integrated optics," *IEEE J. Quantum Electron.*, vol. QE-9, pp. 29–42, Jan. 1973.
[5] C. Elachi, "Waves in active and passive periodic structures: A review," *Proc. IEEE*, vol. 64, pp. 1666–1698, Dec. 1976.
[6] T. Tamir, *Integrated Optics*. Berlin, Germany: Springer, 1975, ch. 3.
[7] T. E. Rozzi, "Rigorous analysis of the step discontinuity in a planar dielectric waveguide," *IEEE Trans. Microwave Theory Tech.*, vol. MTT-26, pp. 738–746, Oct. 1978.
[8] ——, "Network analysis of strongly coupled transverse apertures in waveguide," *Int. J. Circuit Theory Appl.*, vol. 1, pp. 161–178, June 1973.
[9] ——, "The radiation of d.h. stripe-geometry lasers," to be published.
[10] ——, "The spectrum of multilayer planar dielectric waveguides, its discrete representation and applications," to be published.
[11] I. Stakgold, *Boundary Value Problems of Mathematical Physics, Vol. I*. London, England: McMillan, ch. 3, pp. 245–250.